

# Study of lattice defects in BaF<sub>2</sub> using positron annihilation and X-ray diffraction methods at elevated temperatures

TP Jili<sup>1,2</sup>, E Sideras-Haddad<sup>2</sup>, D Wamwangi<sup>2</sup>, D. Billing<sup>2</sup>, C. Ndlangamandla<sup>1</sup> and M. Khulu<sup>1</sup>

<sup>1</sup>Physics Department, University of Zululand, P/B X1001, Kwadlangezwa, 3886, South Africa

<sup>2</sup>School of Physics, University of the Witwatersrand, P/B 3, Wits, 2050, South Africa

E-mail: jilip@unizulu.ac.za

**Abstract.** Different experimental techniques have clearly demonstrated that the predominant intrinsic point defects in ionic barium fluoride are anion Frenkel pairs. We utilized positron annihilation technique in obtaining Doppler broadening spectra in the temperature range 300 – 900 K in which the ratios of the central annihilation areas to the total area of the annihilation curves (S-parameters) are extracted. Generalized gradient approximation in the framework of local density functional theory is used to calculate the Doppler broadening spectra. We found that the positrons annihilations with barium valence electrons, especially 5p and 6s electrons, contribute immensely in the electron-positron annihilation momentum density. The rate of disordering of fluorine sub-structure is found to increase non-linearly from a temperature of 580 K without observing any appreciable ionic conductivity. X-ray diffraction method provided a lattice constant of  $(0.6292 \pm 0.003)$  nm at 693 K, corresponding to the S-parameter of 0.5091, through which an appreciable ionic conductivity of  $4.64 \times 10^{-7} \text{ Ohm}^{-1} \text{ cm}^{-1}$  is first observed. This is demonstrated through the correlation between the lattice constants and the ionic conductivity values at elevated temperatures.

## 1. Introduction

Alkaline-earth fluorides of space group Fm3m have demonstrated interesting properties and they constitute a wide range of applications. Barium fluoride and calcium fluoride exhibiting a wide band gap, are strongly ionic and have been studied partly because of their use in precision vacuum ultraviolet lithography [1], in fast scintillation detection and also in crystalline lens material for precision in vacuum ultra violet optics [2,3]. Han *et al* [4] have recently studied the light output from barium fluoride with the aim of reducing the intensity of a slow component (~310 nm) with a decay constant of around 630 ns which hinders fast timing experiments

Barium fluoride is an ionic conductor whose electrical properties are strongly dependent on temperature because of the migration of anion interstitials. Anion Frenkel pairs and ionic transport is understood through the migration of both anion vacancies and anion interstitials [5,6]. Figueroa et al [7] investigated two possible diffusion mechanisms for fluorite lattice, involving interstitial ions, namely the direct interstitial mechanism and the non-collinear interstitialcy mechanism. They concluded that non-collinear interstitialcy is more probable as it requires much smaller energy to produce ionic displacements.

The present paper explores and demonstrates that at elevated temperatures (well below the melting point) the anion vacancy and the anion interstitial (Frenkel pairs) can well exist without any notable change in ionic conductivity. This is investigated by positron annihilation technique both experimentally and theoretically by obtaining the S-parameters in the temperature range. The lattice parameter as a function of temperature, which plays a pivotal role in the calculation of S-parameters, is obtained from the measured X-ray diffraction patterns

## 2. Method of calculation

Local density approximation (LDA) does not depend on the variation of charge density and this tends to overestimate the correlation energies and thus affecting the calculation of the enhancement factor. This deficiency in LDA is corrected through the generalized gradient approximation (GGA). The MIKA Doppler code (8) used in this work, corrects this deficiency through the enhancement function

$$g_{GGA} = 1 + (g_{LDA} - 1)e^{-\alpha\epsilon} \quad (1)$$

where  $\alpha$  is an adjustable parameter designed to give better annihilation rates. In our case  $\alpha$  is set at 0.22. Note that  $\alpha = 0$  gives the LDA enhancement factor.  $\epsilon$  (the variation in electron charge density) is given by

$$\epsilon = \frac{|\nabla n_-|^2}{(n_{-qtf})^2} \quad (2)$$

where  $n_{-qtf}$  is the local Thomas-Fermi screening length and  $\nabla n_-$  is the change in the electron density. The Arponen –Parjane enhancement function [9] given by

$$g_{LDA-AP} = 1 + 1.23r_s - 0.0742r_s^2 + \frac{1}{6}r_s^3 \quad (3)$$

is substituted in equation (1) for GGA enhancement factor.  $r_s$  is the measure of the density of the system and is the radius of a sphere whose volume equals the volume per electron. Momentum distributions are calculated separately for each electronic state described by  $\psi_j$  as

$$\rho_j(\mathbf{p}) = \pi r_o^2 c u_j^2(0) \left| \int d\mathbf{r} e^{-i\mathbf{p}\cdot\mathbf{r}} \psi_+(\mathbf{r}) \psi_j(\mathbf{r}) \right|^2 \quad (4)$$

where  $u_j$ ,  $\psi_+$  and  $\psi_j$  are the state dependent enhancement factors, positron wavefunction and electron wavefunction respectively.  $r_o$  is the classical radius of electron.

The total electron-positron momentum density within the GGA is obtained by summing partial enhancement factors in equation (4) as

$$\rho(\mathbf{p}) = \pi r_o^2 c \sum_j \gamma_j \left| \int e^{-i\mathbf{p}\cdot\mathbf{r}} \psi_j(\mathbf{r}) \psi_+(\mathbf{r}) d\mathbf{r} \right|^2 \quad (5)$$

S-parameter which is defined as the ratio of central annihilation area to the total annihilation area, is calculated from the electron-positron momentum density as

$$S = \frac{\int_0^{p_z} f(p_z) dp_z}{\int_0^\infty p_z dp_z} \quad (6)$$

where the numerator is the central annihilation area and the denominator denotes the total annihilation area.  $f$  is the positron-electron momentum density function. The momentum window used in our theoretical and experimental calculations is  $(0-3) \times 10^{-3} m_o c$ .

### 3. Experiment

Positron source ( $^{22}\text{NaCl}$ ) sealed between two electron-welded nickel foils, each of thickness  $7\ \mu\text{m}$ , with activity of  $15\ \mu\text{Ci}$ , was sandwiched between two equal samples of barium fluoride each of dimensions  $10\ \text{mm} \times 8\ \text{mm} \times 2\ \text{mm}$ . The coincidence circuit diagram showing detector positions is shown in figure 1.

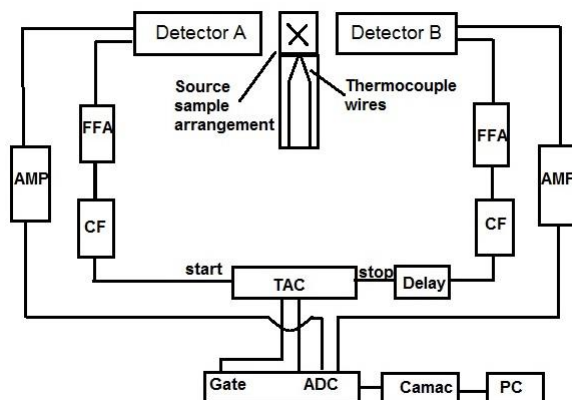


**Figure 1.** Circuit diagram showing two-detector system was employed. The two detectors measured the electron-positron annihilation radiation ( $511 \pm \Delta E$ ) KeV at defects and in bulk.

A K-type (Chromel-alumen) thermocouple was utilized to obtain the temperature of the source-sample sandwich arrangement. A standard coincidence arrangement, in which two high purity germanium detectors (HPGe) with energy resolution of  $1.4\ \text{keV}$  (FWHM) at  $511\ \text{keV}$ , was employed.

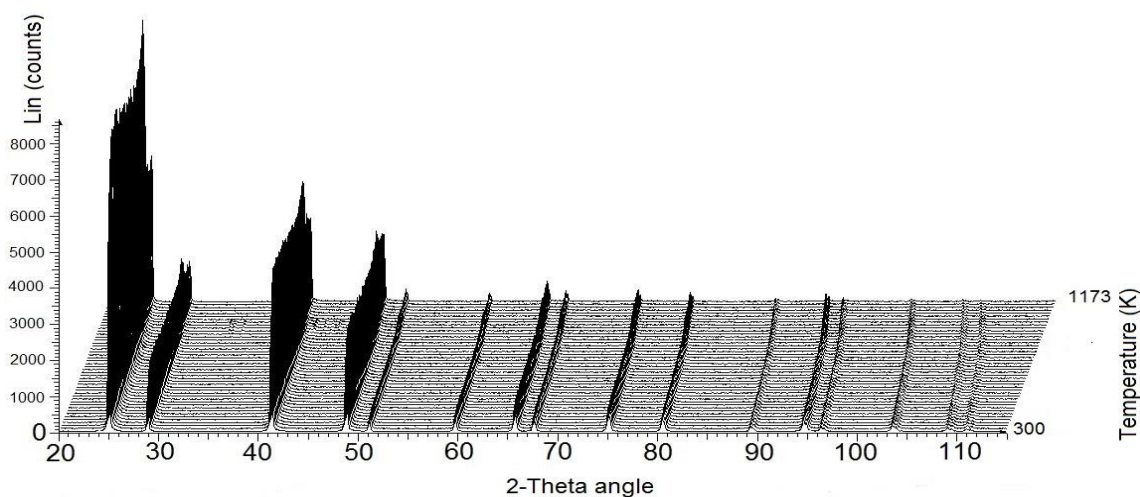


**Figure 2.** Measured X-ray diffraction patterns in  $\text{BaF}_2$  in the temperature range  $300 - 1173\ \text{K}$ .

Two detectors are separated by a distance of  $10\ \text{cm}$  in a collinear arrangement. Accumulation average rate of about  $300\ \text{counts/second}$  was achieved. The peak-to-background of  $\sim 10^4$  was achieved. Source-sample-heater system was kept at a pressure of  $2 \times 10^{-5}\ \text{Torr}$ . Doppler broadening spectra at different temperature values were obtained following the background subtraction. A source correction

was conducted since (10-15) % of the annihilations occurs in the source material and in the foils. Additional lifetimes and intensities corresponding to source and foil were subtracted.

In order to obtain lattice parameters at elevated temperatures, an X-ray diffraction (XRD) method using Bruker D8 Advance, equipped with a Goebel Mirror for pseudo parallel beam optics, a Vantec detector and an Anton Paar XRK-900 reaction chamber was employed. Diffractometer utilizes Cu-K $\alpha$  radiation. A collected X-ray diffraction pattern of [111] barium fluoride in the temperature range 300 – 1173 K is represented in figure 2. The data represents 45 scans from 300 K to 1173 K at regular temperature intervals of 30 K. The XRD patterns were then compared with the reference pattern from Inorganic Crystal Structure Database – Karlsruhe (ICDS) [10].

Rietveld refinement was performed using TOPAS 4.2 and EVE programs to extract lattice parameters as a function of temperature. Lattice parameters obtained at different temperatures were then incorporated in the theoretical calculations of positron-electron annihilation momentum density using MIKADoppler program.

#### 4. Results and discussion

The formation energy for fluorine vacancy (F $^-$  - vacancy) is -1.06 eV, which is more negative than the formation energy for Ba $^{2+}$  vacancy, which is positive at 21.27 eV [11]. Therefore the migration of an anion is energetically preferred to that of a cation and throughout the experiment, in the temperature range 300-800 K, anion vacancy formation is considered. For interstitial formation energies, the octahedral sites in face-centered cube fluorites are the most stable sites for anion and cation interstitials [12] a fact we took into consideration in this work.

X-ray diffraction analysis was performed on barium fluoride over a temperature range, 300-1173 K, below the melting point in order to deduce the variation of the lattice constant with temperature as shown in figure 3.

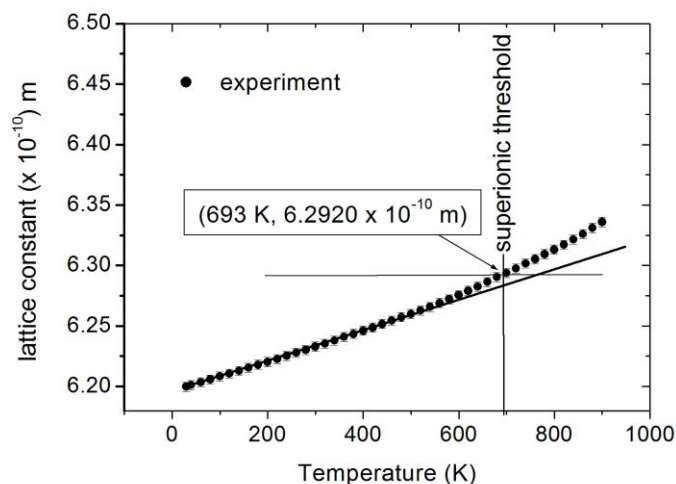


**Figure 3.** Variation of lattice constant in BaF $_2$  as a function of temperature.

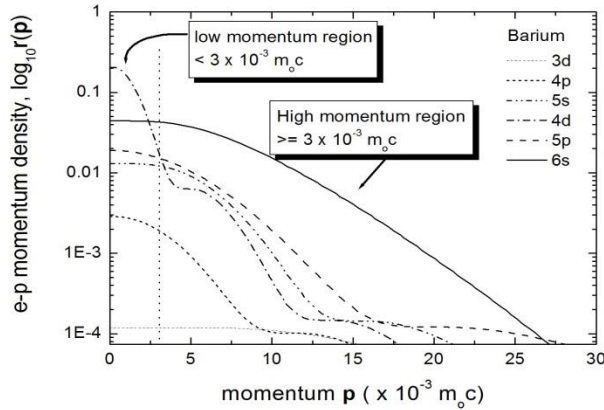


**Figure 4.** Barium decomposition shows two regions of interest. Most positron annihilations take place with low momentum electrons in the region  $0 < p \leq 3 \times 10^{-3} m_0c$ .

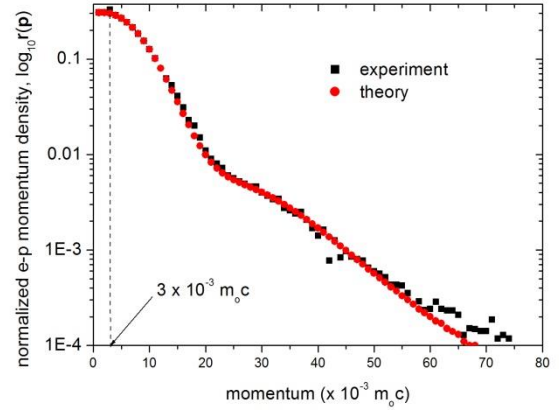


**Figure 5.** Low momentum window  $0-3 \times 10^{-3} m_0c$  is chosen for both theory and experiment for consistency

In the temperature range between 300 – 580 K, we observe a linear behaviour of lattice constant as a function of temperature. In contrast, between 580 K and 1173 K, a non-linear behaviour of the lattice constant becomes evident. Our extracted experimental values of the lattice parameters compare well with other values in the relevant literature [12-14]. Each lattice constant extracted from XRD measurements in the temperature range is used to construct a supercell.

Partial electron-positron annihilation momentum distributions are derived from equation 4 and are shown in figure 4. The GGA in the framework of density functional theory (DFT) confirms that most contributors towards electron-positron annihilation momentum density are the low momentum Ba-5p valence electrons rather than Ba – 6s electrons as shown in figure 4. The total momentum distribution is calculated from equation 5 and compares well with experimental e-p momentum density as shown in figure 5. Normalized electron-positron momentum densities were then experimentally obtained at different temperature values. For each spectrum, a fixed momentum window,  $0 < p \leq 3 \times 10^{-3} m_0c$  (low momentum range) around the centroid of the photopeak was used for both experimental and theoretical spectra for the calculation of S-parameters as shown in figure 6. The deviation of experimental S-parameter values from a theoretical values commencing at about 600 K is not of major concern since both experiment and theory deviate from an observed linear behaviours at about the same temperature (lattice constant). The deviation is probably due to the tail of specific heat anomaly which begins between 600 and 700 K and which is not incorporated in the MIKA code. This is interpreted as a transition from a normal fluorite structure at low temperatures to highly disordered state in which  $F^-$  ions are distributed between normal anion and interstitial sites.

Using positron annihilation parameters, there is an agreement between the theory and the experiment regarding thermal value at which both S-parameters (experiment and theory) begin to deviate from linear behaviour as shown in figure 6. The ionic conductivity measurements shown in figure 7 in relation to figure 3 suggest that a small threshold ionic conductivity (or a small noticeable disordering of F- sub-lattice), as probed by positrons, appears at the threshold lattice constant and temperature of  $a_0 = 0.6292$  nm and  $T = 693$  K respectively. This minimum anionic interstitial transportation takes place at octahedral sites of the sample.

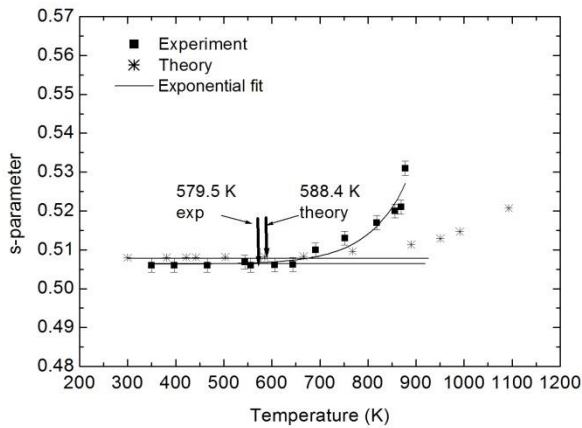


**Figure 6.** Comparison between theory and experiment. The experimental large deviation of S-parameter which begins at  $\sim 579.5$  K compares well with a theoretically calculated deviation

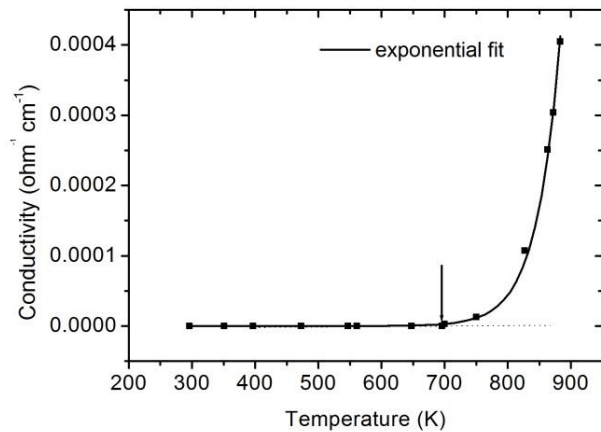


**Figure 7.** Measured ionic conductivity as a function of temperature. The minimum threshold temperature for ionic conduction is  $\sim 693$  K corresponding to the conductivity of  $4.64 \times 10^{-7}$  ohm $^{-1}$ cm $^{-1}$ .

## 5. Conclusion

Using both the positron annihilation and X-ray diffraction techniques, we found that the annihilation fractions of positrons interacting with low momentum electrons slightly differ with an increase of temperature. We also observed that creating an anion di-vacancy can largely increase the annihilation fractions with barium low momentum electrons due to an increase of intensity of positron wavefunction around barium atom. It was of no interest to consider cationic Frenkel defects since in reality the formation energy (21.27 eV) is very large and positive compare to the Fermi gap energy ( $\sim 10$  eV). We also see that charged anionic Frenkel interstitials are more stable than neutral anion Frenkels and that the minimum lattice constant required to establish a noticeable anion Frenkel defects formation is 0.62341 nm at  $\sim 580$  K. The minimum ionic conductivity at octahedral sites occurs at threshold lattice constant of 0.62920 nm (corresponding to a temperature of 693 K).

## Acknowledgement

We gratefully acknowledge financial support from the Research Committee of the University of Zululand and School of Physics at the University of the Witwatersrand.

## References

- [1] Levin ZH, Burnett JH and Shirley EL 2003 *Phys. Rev.* **B68** 155120
- [2] Levin ZH, Burnett JH and Shirley EL 2004 *Phys. Rev.* **B70** 239904
- [3] Katsika-Tsigourakou JV and Skordas E 2010 *Cent. Eur. Phys.* **8** 900-904
- [4] Han H, Zhang Z, Weng X, Liu J, Guan X, Zhang K and Li G 2013 *Rev. Sci. Instrum.* **84** 7073503
- [5] Chandra S 1981 *Superionic Solids : Principles and Applications* (North Holland, Amsterdam)
- [6] Liliard AB, Hayes W (Ed) 1974 *Crystals with Fluoride Structure* (Clarendon Press, Oxford)
- [7] Figueroa DR, Chadwick AV and Strange JH 1978 *J. Phys. C: Solid State Physics* **11** 55-73
- [8] Hakala T 2001 *Special Assignment*, Helsinki University of Technology, Espoo
- [9] Barbiellini B, Puska MJ, Torsti T and Nieminen RM 1995 *Phys. Rev.* **B51** 7341
- [10] ICDS: FIZ – Karlsruhe-Leibniz Institute for Information Infrastructure
- [11] Bollman W 1981 *Cryst. Res. Technol* **16** 9 1039-1050
- [12] Lie K, Xiao HY and Wang LM 2008 *Nuclear Instruments and Methods* **B266**, 2698
- [13] Leger JM, Haines J, Atouf A, Schulte O and Hull S 1995 *Phys. Rev.* **B52**, 13247
- [14] Nyawere P, Scandolo S, Makau M and Amolo G 2014 *Solid State Communications* **179**, 25-28